Changing pattern of drought in Nepal and associated atmospheric circulation

Article *in* Atmospheric Research · August 2021

DOI: 10.1016/j.atmosres.2021.105798

7 authors, including:

Kalpana Hamal
Institute of Atmospheric Physics
21 PUBLICATIONS **106** CITATIONS
SEE PROFILE

Shankar Sharma
Central Department Of Hydrology & Meteorology
27 PUBLICATIONS **141** CITATIONS
SEE PROFILE

Binod Pokharel
Utah State University
28 PUBLICATIONS **251** CITATIONS
SEE PROFILE

Dibas Shrestha
Tribhuvan University
36 PUBLICATIONS **474** CITATIONS
SEE PROFILE

Contents lists available at ScienceDirect

Atmospheric Research

journal homepage: www.elsevier.com/locate/atmosres

Changing pattern of drought in Nepal and associated atmospheric circulation

Kalpana Hamal [a, b], Shankar Sharma [c], Binod Pokharel [c, d], Dibas Shrestha [c], Rocky Talchabhadel [e], Alen Shrestha [f], Nitesh Khadka [b, g, h, *]

[a] International Center for Climate and Environment Sciences, Institute of Atmospheric Physics, Chinese Academy of Sciences, P.O. Box 9804, Beijing 100029, China
[b] University of Chinese Academy of Sciences, Beijing 100049, China
[c] Central Department of Hydrology and Meteorology, Tribhuvan University, Kirtipur, Nepal
[d] Utah Climate Center, Department of Plants, Soils, and Climate, Utah State University, Logan, UT, USA
[e] Texas A&M AgriLife Research, Texas A&M University, El Paso, TX 79927, USA
[f] FTN Associates, 3 Innwood Circle, Suite 220, Little Rock, AR, 72211, USA
[g] Institute of Mountain Hazards and Environment, Chinese Academy of Sciences, Chengdu 610041, China
[h] Siddhartha Environmental Services, Kathmandu, Nepal

ARTICLE INFO

Keywords:
Drought
Standardized Precipitation Evaporation Index (SPEI)
Decadal variation
Atmospheric circulation
Nepal

ABSTRACT

Understanding the spatial and temporal characteristics of drought is vital for the agricultural, hydrological, ecological, and socio-economic systems. This study investigates the spatial and temporal variation of drought characteristics in Nepal using the Standardized Precipitation Evapotranspiration Index (SPEI) based on observational monthly temperature and precipitation data from 1987 to 2017. The drought variation was observed in the Western, Central, and Eastern regions of Nepal at short-term (SPEI4) and long-term (SPEI12) timescales, revealing the increased drought frequency, duration, and severity in the recent decade. The frequency of short-term drought (SPEI4 ≤ -1) has elevated by 15%, 17%, and 15% in Western, Central, and Eastern regions, respectively, during 2005–2017 compared to 1987–2004. Moreover, the interdecadal increase of drought characteristics was prominent after 2004, revealed by the SPEI12 with aggravated and prolonged drought episodes. The summer drought index (SPEI4-Sep) showed an interannual variation in the Western region at a seasonal timescale, whereas decadal variation in the Central and Eastern regions. Meanwhile, summer drought events increased five times in the Central region, two times in the Eastern Region, and did not observe any change in the Western region after 2004. The large-scale atmospheric circulations revealed the negative summer precipitation anomalies due to weakening wind anomalies with anti-cyclonic circulation and moisture divergence over the Indo-Gangetic plain and Nepal, respectively, leads to enhanced drought after 2004. Furthermore, the moisture transport from the Arabian Sea and the Bay of Bengal to the study region is weaker, resulting in more drought events, especially in the Central and Eastern regions.

1. Introduction

In the context of climate change, frequent and severe drought, as well as heatwave episodes, have been well documented globally (Reichstein et al., 2013; Trenberth et al., 2014), which has dragged many countries into vulnerability, affecting the meteorological, agricultural, hydrological, and socio-economic systems (Haile et al., 2020; Wilhite and Glantz, 1985). The precipitation deficit develops a meteorological drought, whereas insufficient precipitation and water scarcity lead to agricultural and hydrological droughts (Herrera-Estrada et al., 2017; Wang et al., 2016). The prolonged meteorological drought creates insufficient soil moisture for plants, affecting the plant growth adversely, resulting in agricultural drought (Fahad et al., 2017; Hamal et al., 2020c; Shen et al., 2019). Meteorological and agricultural droughts increase stress to the surface, subsurface, and groundwater resources, further evolving the hydrological drought (Haile et al., 2020). The prolonged and aggregated meteorological, agricultural, hydrological droughts lead to stark socio-economic consequences (Guo et al., 2019).

Several drought indices have been developed to assess the drought types and characteristics with the inclusion of climatic variables, such

* Corresponding author at: Institute of Mountain Hazards and Environment, CAS 9, Block 4, Renminnanlu Road, Chengdu, China.
E-mail addresses: kalpana@mail.iap.ac.cn (K. Hamal), sharma.sh969@gmail.com (S. Sharma), binod52@gmail.com (B. Pokharel), st.dibas@yahoo.com (D. Shrestha), rocky.ioe@gmail.com (R. Talchabhadel), nkhadka@imde.ac.cn (N. Khadka).

https://doi.org/10.1016/j.atmosres.2021.105798
Received 2 March 2021; Received in revised form 21 June 2021; Accepted 1 August 2021

as precipitation, temperature, and soil moisture (Mishra and Singh, 2010; Zargar et al., 2011). Standardized Precipitation Index (SPI) can be calculated over different timescales using only precipitation data (McKee et al., 1993). Palmer Drought Severity Index (PDSI) uses precipitation and temperature variables to calculate water balance on fixed timescales (; Palmer, 1965). Meanwhile, the Standardized Precipitation Evapotranspiration Index (SPEI) also considers precipitation and temperature for drought calculation at multiple timescales and is useful to monitor and identify meteorological, agricultural, hydrological, and social droughts (Vicente-Serrano et al., 2010). SPEI overcomes the limitation of SPI and PDSI as it computes the drought in different timescales, has a simple methodology, and provides robust results (Liu et al., 2018; Vicente-Serrano et al., 2010). SPEI has been successfully applied in the South Asian region for capturing the areal extent and severity of drought in district and sub-basin levels (Aadhar and Mishra, 2017). Moreover, Kumar et al. (2013) used the SPEI at various timescales to examine changes in summer drought in India to explore the effects of climate change.

Nepal, a central Himalayan country, is located in the South Asian Monsoon region, suffering from increased drought severity (Aadhar and Mishra, 2017; Miyan, 2015). Few previous studies have derived the spatial and temporal characteristics of drought in Nepal (Dahal et al., 2015; Kafle, 2015; Khatiwada and Pandey, 2019; Sigdel and Ikeda, 2010; Wang et al., 2013); however, the mechanism of the winter drought is only described by Wang et al. (2013). Sigdel and Ikeda (2010) analyzed the drought in Nepal during 1971–2003, whereas Dahal et al. (2015) analyzed the drought in Central Nepal during 1981–2013. Both studies used the SPI to reveal the increased severity and frequency of drought with a substantial interannual variation. Khatiwada and Pandey (2019) have portrayed a better performance of SPI among several other indices to characterize drought in the Karnali basin of Nepal, even though there was an issue of missing data. A local-scale drought study in far-western Nepal showed increased drought severity using the Standardized Reconnaissance Drought Index; however, it did not find any significant correlation with temperature and precipitation (Kafle, 2015). In contrast, Baniya et al. (2019) used satellite-derived Vegetation Condition Index (VCI) in Nepal and reported the decreased droughts on an annual and seasonal scale during 1982–2015. Further, Panthi et al. (2017) used a dendrochronological approach to reveal the spring (March–May) drought in the central Himalaya from the past three centuries. Recently, Hamal et al. (2020c) assessed the drought impacts on the summer maize and winter wheat cropping cycle using SPEI and detected the turning point of drought in 2000. Moreover, Sharma et al. (2021a) linked the seasonal and annual drought calculated from SPI with climatic indices and provided evidence on the increasing drought frequency and severity in recent years. Nevertheless, most of the past studies have analyzed the long-term drought characteristics at seasonal and interannual timescales in Nepal based on precipitation as a key variable. So far, the changes in drought characteristics and their associated mechanisms have not been explicitly studied.

The South Asian Summer Monsoon (SASM) variation frequently manifests drought and flood episodes in the South Asian countries (Krishnamurthy and Shukla, 2000; Mallya et al., 2016; Kumar et al., 2013). Several previous studies have shown the increased drought intensity and frequency affecting different parts of South Asia in recent decades (Mallya et al., 2016; Kumar et al., 2013). Specifically, from the beginning of the 21st century, the effects are more pronounced with decreasing monsoon precipitation due to atmospheric circulation change (Ma et al., 2019). The dryness has increased over the Indo-Gangetic Plain and northeast India in recent years (2001–2018) (Maharana et al., 2021). For instance, 2015 was recorded as the third driest year with a 25.8% monsoon deficit over the Indo-Gangetic Plain (Mishra et al., 2016), which appeared to be the recent severe summer drought. In the same year, drought significantly impacted the yield of major crops that causes food insecurity for 80% of the population in Western Nepal (Gyawali, 2016). Similarly, recent studies also showed the drought frequency has varied over different regions of Nepal and increased mainly after the 2000s (Hamal et al., 2020c; Sharma et al., 2021a); however, atmospheric circulation related to drought change has not been documented yet.

The variations of large-scale atmospheric circulation patterns are closely related to occurrences of extreme events (i.e., floods and drought) (Omidvar et al., 2016; Vicente-Serrano, 2006). In recent decades, the variation in SASM is associated with low-level wind change over the Indo-Pacific region, weakening the El Niño transfer mechanism (Feba et al., 2019). The weakened SASM circulation leads to decadal-scale drought conditions (Hernandez et al., 2015). Moreover, there is a difference in the atmospheric circulation (wind and moisture flux) pattern of the Indian monsoon during the reference period (1971–2000) and recent period (2001–2018), which has influences on the distribution of precipitation and shifting the dry/wet zones over the Indian region (Maharana et al., 2021). Further, Jin and Wang (2017) and Roxy et al. (2015) also showed the strengthening of the SASM in the recent decade due to the differential warming rate over land and the surrounding ocean. However, the Indo-Gangetic plains and northeast India were experiencing a dry summer due to the decline in the wind strength and restricted the atmospheric moisture availability during 2001–2018 (Maharana et al., 2021). These are the important features observed in the summer season over the Indian region; therefore, study on the large-scale circulation change that determines the spatial and temporal variation of summer drought over the southern slope of Central Himalaya, Nepal, is necessary.

More specifically, the objectives of the current study are to (i) analyze the spatial and temporal variation of drought over different regions of Nepal using SPEI calculated from long-term observed datasets (1987–2017) and (ii) study the atmospheric circulation patterns that

cause such variation using a high-resolution reanalysis dataset. The analysis of drought characteristics across Nepal and its underlying mechanism would greatly help society and policymakers for effective drought mitigation, adaptation, and reducing future drought risks.

2. Materials and method

2.1. Study area

Nepal is a South Asian Himalayan country located between 26.36°N–30.45°N and 80.06°E–88.2°E, encompassing an area of 147,516 km^2 (Fig. 1a). Within such a relatively small latitudinal range (140–250 km), the elevation rises from 60 m above sea level (asl) in the south to 8848 m asl at the summit of Mt. Everest in the north. The two large-scale weather systems, i.e., SASM and westerly wind system, play an essential role in governing the climatology of the country (Sharma et al., 2020b; Talchabhadel et al., 2018). The climate varies with the topography, ranging from tropical savannah in the lowland to polar frost in the Himalayas (Karki et al., 2017). The four climatic seasons are pre-monsoon (March–May), summer monsoon (June–September), post-monsoon (October–November), and winter (December–February) that are classified based on precipitation and temperature. The annual precipitation cycle reveals that the summer season (JJAS) receives the highest proportion (~80%) of precipitation, whereas other seasons receive 20% of precipitation (Sharma et al., 2020d). In summer, the strong southeasterly monsoonal wind flow and strengthening monsoonal trough are related to high precipitation (Sharma et al., 2020b). The strong southeasterly (northwesterly) wind anomalies supply more (less) moisture from the Arabian Sea and Bay of Bengal to Nepal during the winter season, which often attributes to wet (dry) years (Hamal et al., 2020a). Moreover, topography plays a major role in precipitation distribution over the different regions of Nepal (Hamal et al., 2020b; Karki et al., 2017; Sharma et al., 2021b).

The air temperature varies in the country on an altitudinal basis, i.e., high in the southern lowlands and gradually decreases towards the northern highlands (MoFE, 2019). The highest temperature is observed in the pre-monsoon, summer, post-monsoon, and winter seasons, respectively (MoFE, 2019). For this study, Nepal is divided into Western, Central, and Eastern regions based on the length and timing of the summer monsoon over these regions (Kansakar et al., 2004) (Fig. 1a). Moreover, the Western, Central, and Eastern regions are the drainage basins for Karnali, Gandaki, and Koshi rivers, respectively.

2.2. Data

More than 300 climatological stations in Nepal are maintained by the Department of Hydrology and Meteorology (DHM), Government of Nepal (www.dhm.gov.np). Most of these stations are established after 2000 and do not feature long-term climate data (Chen et al., 2021). Moreover, the stations are unevenly distributed, denser in the southern region (below 2500 m elevation), and sparse over the northern mountainous region (Sharma et al., 2020a). First, we screened all available climatological stations, which recorded both temperature and precipitation data. Secondly, stations that featured less than 90% of daily climatological data (precipitation and temperature) annually during 1987–2017 were discarded. After this quality control, only 38 stations were found to feature continuous temperature and precipitation records for the study period (1987–2017) with optimal spatial coverage, which were used in this study (Fig. 1a). Then, these were converted into monthly datasets by averaging the daily datasets. The monthly average precipitation and temperature of three different regions during the study period are presented in Fig. 1(b, c, and d). Regionally, West-

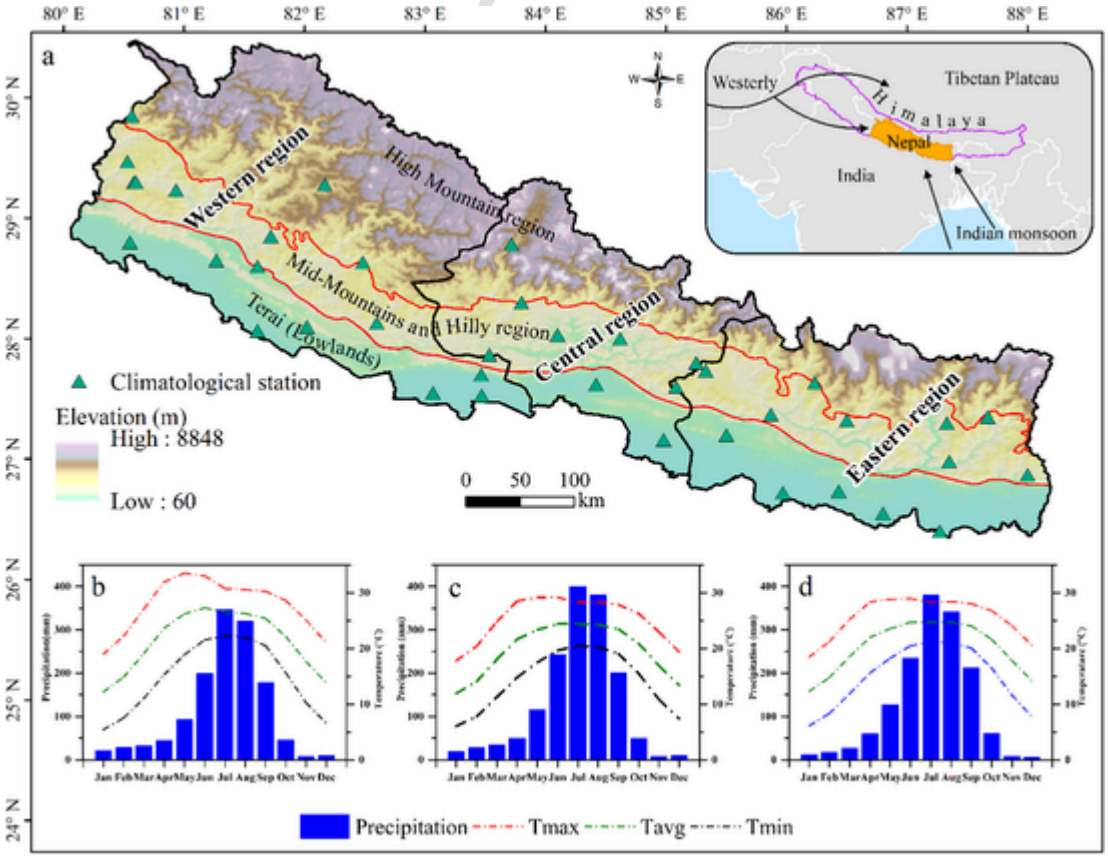

Fig. 1. (a) The study area, Nepal, with 38 climatological stations used across the Western, Central, and Eastern regions. Lower panel graphs show the seasonal cycle of average precipitation and air temperature of (b) Western, (c) Central, and (d) Eastern regions during 1987–2017.

ern, Central, and Eastern Nepal featured 16, 10, and 12 stations, respectively (Fig. 1a). The seasonal cycle of precipitation shows the highest proportion of precipitation in the summer (JJAS), followed by pre-monsoon (MAM), post-monsoon (ON), and winter (DJF) seasons. The temperature peaks are between March and July, generally making them the hottest months (Figs. 1b, c, and d).

Additionally, we used a recently released ERA5 (C3S, 2017) reanalysis dataset developed by the European Centre for Medium-Range Weather Forecasts (ECMWF) to analyze atmospheric circulation patterns. The ERA5 datasets that are used in this study include total monthly precipitation, zonal (u) and meridional (v) winds at 850 hPa, and Vertically Integrated Divergence Moisture flux (VIDMF) with the spatial resolution of 0.25° × 0.25°. Recently, Sharma et al. (2020b) validated the ERA5 precipitation product using an extensive gauge network (220) of Nepal during 1987–2015, revealing that ERA5 is a good alternative for precipitation monitoring in the country. The already calculated South Asian Summer Monsoon (SASM) index is used in this study, which can be freely downloaded from the website: http://ljp.gcess.cn/dct/page/65576.

2.3. Methodology

2.3.1. Calculation of SPEI

Standardized Precipitation Evapotranspiration Index (SPEI) is a drought index that uses the time series of precipitation (P_i) and potential evapotranspiration (PET_i). The precise method of SPEI calculation is given by Vicente-Serrano et al. (2010). SPEI calculation is based on the water balance (D_i), which is the difference between precipitation and potential evapotranspiration as given in Eq. 1.

$$D_i = P_i - PET_i \quad \text{here } i = 1, 2, 3.. \ldots \ldots n \tag{1}$$

Different methods are available for estimating PET_i that can be used based on data availability for different climatic parameters (Mavromatis, 2007). In this study, we adopted the Thornthwaite method (Thornthwaite, 1948) that has been widely used in previous studies in the Asian region (Talchabhadel et al., 2019; Van der Schrier et al., 2011) and requires only temperature data. On the other hand, the Penman-Monteith method is one of the complex methods for calculation of PET_i, which requires several variables (vapour pressure, soil moisture, air temperature, wind speed, cloud cover, and precipitation) (Allen et al., 1998; Shrestha et al., 2020a; Shrestha et al., 2020b) that are not available in all stations we considered for this study. Further, Portela et al. (2019) show a strong correlation (≥ 0.95) between the Thornthwaite method and the Penman-Monteith method and suggested using the Thornthwhite method over the Penman-Monteith method.

PET_i and P_i values at different stations over regions recorded in 1987–2017 are averaged, and the regional SPEI of the multi-time scale is obtained. D_i is fitted with the log-logistic distribution function, and then SPEI is calculated for multiple timescales, such as SPEI1, SPEI2, SPEI3, SPEI4…SPEI12. SPEI at different timescales 1–5, 6, and 12-months can be used for the short-term, medium-term, and long-term drought, respectively (Tan et al., 2015; Yang et al., 2016). The SPEI series has both positive and negative values representing the wet condition (SPEI ≥ 1) and dry condition (SPEI ≤ −1), respectively (Beguería et al., 2014; Tan et al., 2015). A threshold value of −1 is used to determine the drought condition, and various drought categories (Vicente-Serrano et al., 2010) are given in Table 1. The occurrence of drought with relatively higher water deficiency conditions (SPEI ≤ −2) is extreme drought. In this study, SPEI4, SPEI4-Sep, and SPEI12 were used to explore drought on short-term, seasonal (monsoonal), and long-term timescales. Technically, SPEI4 is calculated using temperature and precipitation of the current month and the past three months. The precipitation and temperature during June–September are used to calculate the summer drought index (SPEI4-Sep). Similarly, Sharma et al. (2021a) and Aadhar and Mishra (2017) have also used SPI4-Sep and SPEI4-Sep to represent the summer drought over Nepal and India, respectively. Moreover, SPEI12 is calculated with temperature and precipitation of the current month and past 11 months, representing the long-term drought condition or annual drought.

Table 1
Drought classification based on SPEI values.

SPEI value	Drought category
−1.5 < SPEI ≤ −1	Moderate
−2 < SPEI ≤ −1.5	Severe
SPEI ≤ −2	Extreme

2.3.2. Drought characteristics

The drought event (e) is defined as a period in which the SPEI value is within or continuously less than the threshold level (−1) of drought (Tan et al., 2015). After identifying the drought events, drought characteristics like duration and severity are calculated. The drought duration (De) is the number of months between the drought initiation time (t_i) and drought termination time (t_e) (Mishra and Singh, 2010). Severity (Se) is the sum of SPEI values during drought events (Eq. 2).

$$Se = \left(\sum_{i=1}^{n} SPEI \right)_e \tag{2}$$

The frequent occurrences of drought during the study period were assessed from the cumulative curves, which show the probability of the observation that falls below or above the particular threshold level (SPEI ≤ −1) (Eq. 3).

$$F(t) = \frac{1}{N}\sum_{i=1}^{N} 1 \ \left(X_i < t\right) \tag{3}$$

Where N is the number of months in observation, X_i is the number of values less than t, and t is a drought threshold (SPEI ≤ −1).

3. Results

3.1. Spatial and temporal characteristics of drought

The spatio-temporal variation of SPEI over Western, Central, and Eastern regions of Nepal shows the wetness and dryness at different timescales in the last three decades (Fig. 2). Notably, during 1992, 1994, 2008, 2009, 2012, 2015, and 2016 almost all months experienced severe dry conditions. Consequently, the drought frequency occurrences have varied over the different regions from short-term to long-term timescales. In the Western region, drought has frequently occurred during the study period, with consecutive drought events between 2000 and 2007 (Fig. 2a). Moreover, the prolonged and severe drought episodes are observed after 2004, as recorded in 2009, 2010, 2012, and 2015. Fig. 2b shows that the Central region recorded fewer drought events during 1987–2004 (hereafter, P1 period), whereas more prolonged dry episodes after 2004. Similar drought variation was observed in the Eastern region (Fig. 2c), intensifying drought episodes between 2005 and 2017 (hereafter, P2 period). The total drought events in the Western, Central, and Eastern regions during the study period are summarized in Table 2.

The temporal variation of short-term (SPEI4) and long-term (SPEI12) droughts over three different regions are shown in Fig. 3. Frequent consecutive short-term drought events were witnessed in the Western region between 2000 and 2007 (Fig. 3a), whereas the Central and Eastern regions were observed between 2005 and 2017 (Fig. 3c and e). In the Western region, observed 10 and 14 short-term drought events in P1 and P2 periods, respectively, while Central and Eastern regions observed 9 and ~ 14 in the P1 and P2 periods (Table 2). The total number of long-term drought events in the Western region was higher during the P2 period (8 events) than the P1 period (3 events). The long-term drought episodes were six and four times higher over the Central and Eastern region, respectively, in the P2 period compared to the P1 period (Table 2). Even though the frequency of long-term drought events is higher in the Western region in both periods (Fig. 3b), the Central and Eastern regions have suffered a continuous drought in recent periods (Fig. 3d and f).

3.2. Drought Frequency

The cumulative probability of drought in two sub-periods (P1 and P2) at short-term and long-term timescales for three regions of Nepal is shown in Fig. 4. The cumulative frequency of short-term drought for the

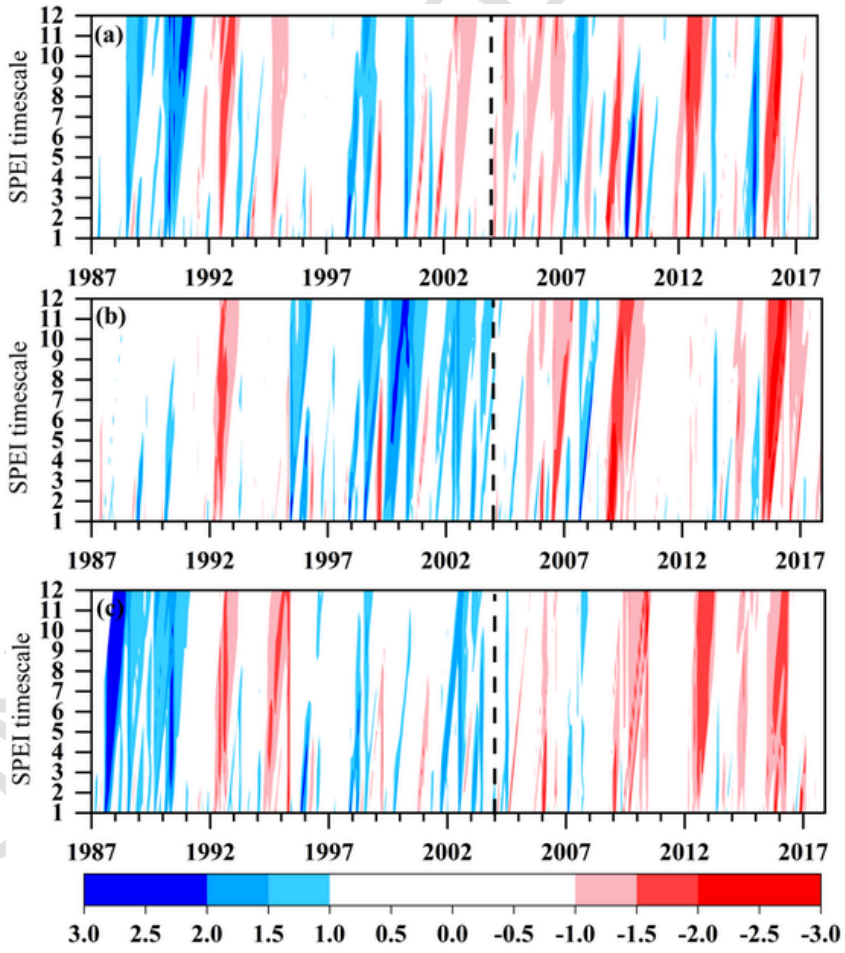

Fig. 2. The temporal variation of the SPEI at different timescales for (a) Western, (b) Central, and (c) Eastern regions of Nepal during 1987–2017. The red and blue value in the colour bar represents the dryness and wetness, respectively. The black dash line separates the drought events before and after 2004. (For interpretation of the references to colour in this figure legend, the reader is referred to the web version of this article.)

Table 2
Total number of the short-term (SPEI4 ≤ −1) and long-term (SPEI12 ≤ −1) drought events over three regions of Nepal. P1, P2, and P represent the period 1987–2004, 2005–2017, and 1987–2017, respectively.

Drought	Western			Central			Eastern		
	P1	P2	P	P1	P2	P	P1	P2	P
Short-term (SPEI4 ≤ −1)	10	14	24	9	13	22	9	14	23
Long-term (SPEI12 ≤ −1)	3	8	11	1	6	7	2	8	10

Western, Central, and Eastern regions increased by 15%, 18%, and 15%, respectively, from P1 to P2 (Fig. 4a, c, and e). However, the different drought categories (moderate, severe, and extreme) occurrences vary in different regions. For example, the moderate short-term drought frequency was almost 2, 3, and 3 times higher in P2 than P1 period, while severe drought frequencies have increased by 4%, 7%, and 3% in the P2 period than P1 period over the Western, Central, and Eastern regions, respectively (Fig. 4 a, c and e). Moreover, the extreme drought increased by 0.6% and 1.3% over Western and Central regions, respectively, whereas no extreme drought was observed over the Eastern region.

The long-term drought has increased during the P2 period than in the P1 period over the Western, Central, and Eastern regions, by 2%, 31%, and 16%, respectively (Fig. 4b, d, and f). For the Western region, long-term drought frequency did not change for moderate, severe, and extreme droughts from P1 to P2 (Fig. 4b), with a difference below 1%. However, in the P2 period, the moderate, severe, and extreme drought in the Central region has increased by 13%, 5%, and 2%, respectively, compared to the P1 period (Fig. 4d). In the Eastern region, moderate and severe droughts were 3 and 1.5 times higher in the P2 period than in the P1 period, whereas extreme drought did not occur in both periods (Fig. 4f).

3.3. Drought duration and severity

The variation of drought duration and severity at short-term and long-term timescales during the P1 and P2 periods is shown in Fig. 5. In all three regions, the total short-term drought duration and severity in the P2 period were almost twice that of the P1 period (Fig. 5a and c). For instance, the total drought duration of 29, 17, and 23 months during the P1 period increased to 49, 44, and 42 months in the P2 period over Western, Central, and Eastern regions, respectively. Moreover, the increase in drought duration had led to the enhanced drought severity in the second period in all three regions.

For the Western region, the total drought duration and severity at long-term timescale were very similar for the two periods (P1 and P2), with a difference in drought duration and severity of only 2 months and − 4, respectively (Fig. 5b and d). In contrast, a significant increase in drought duration and severity was found in the Central and Eastern regions during the P2 period (Fig. 5b and d). For example, in the Central region, the duration (severity) was 10 (−13.8) during the P1 period, which later increased to 50 (−72.8) in the P2 period. This result shows that drought was five-fold longer and severe than that of the earlier period in the Central region (Fig. 5b and d). Similarly, in the Eastern region, the drought was 2.4 times longer and severe than in the P1 period. These results suggest increased drought characteristics (frequency, duration, severity), mainly in the Central and Eastern regions.

3.4. Summer drought variation

For further analysis, we choose a summer season (JJAS), which contributes the highest amount (about 80%, Fig. 1) of precipitation annu-

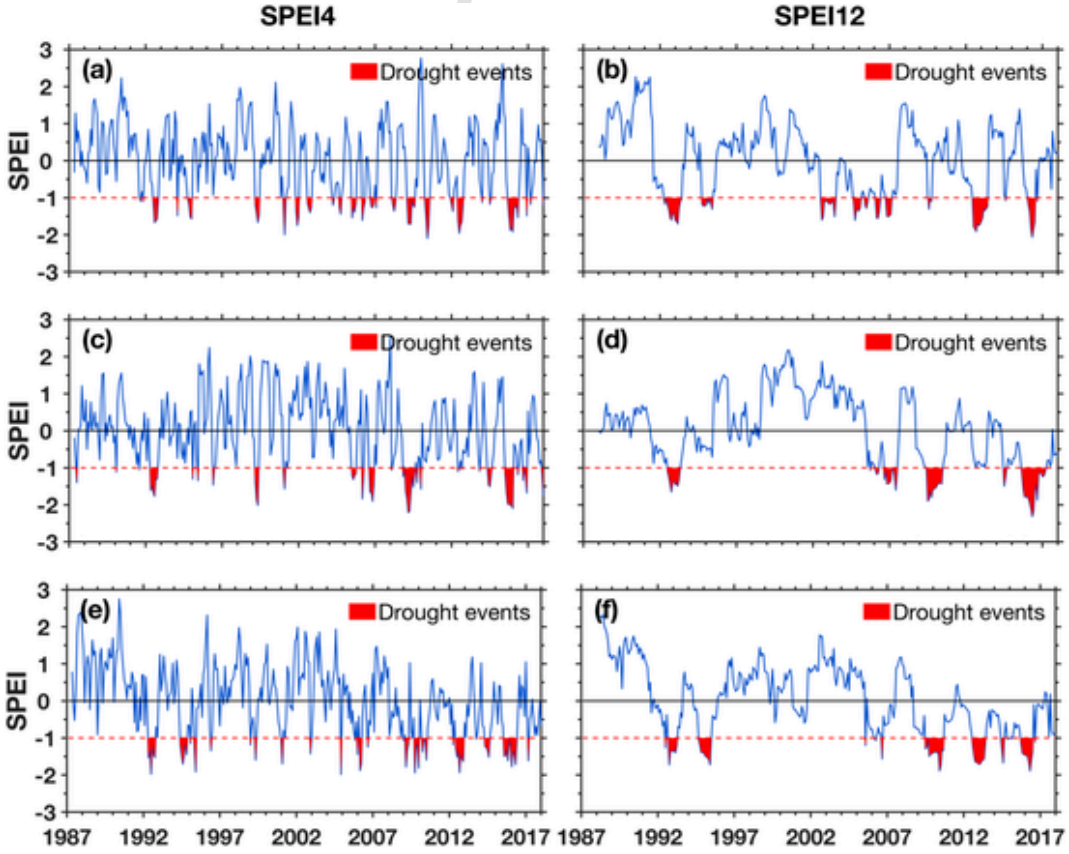

Fig. 3. Temporal variation of SPEI4 and SPEI12 over different regions: (a, b) Western, (c, d) Central, and (e, f) Eastern from 1987 to 2017. The dotted red line represents the threshold level (−1) of drought. (For interpretation of the references to colour in this figure legend, the reader is referred to the web version of this article.)

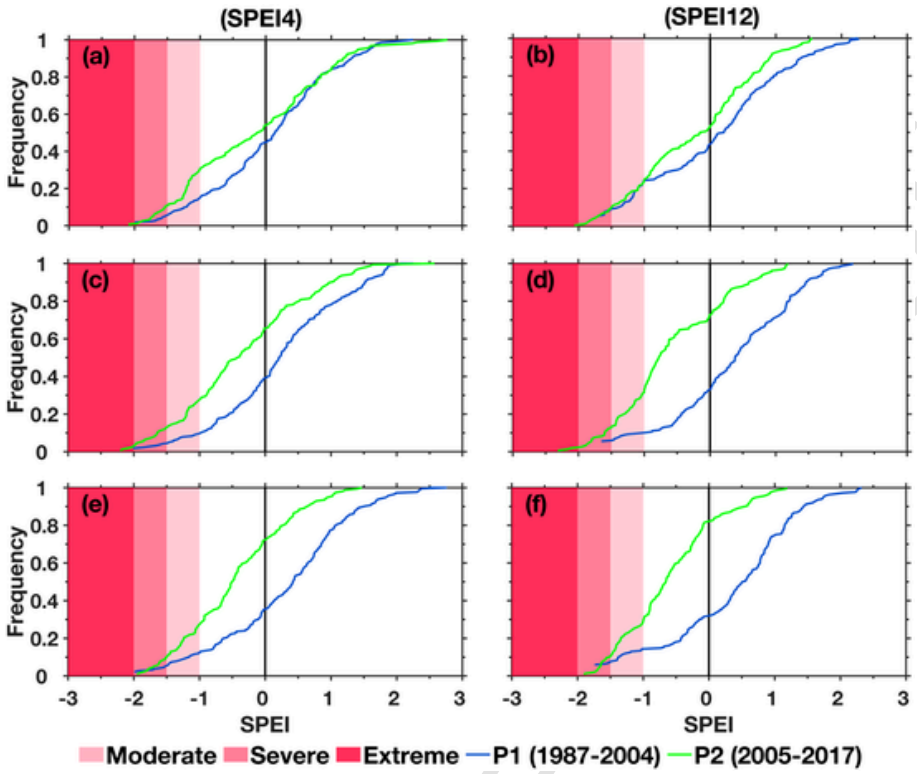

Fig. 4. The cumulative frequency of SPEI4 (left panel) and SPEI12 (right panel) over different regions; (a, b) Western, (c, d) Central, and (e, f) Eastern for the period P1 (1987–2004, blue line) and P2 (2005–2017, green line). (For interpretation of the references to colour in this figure legend, the reader is referred to the web version of this article.)

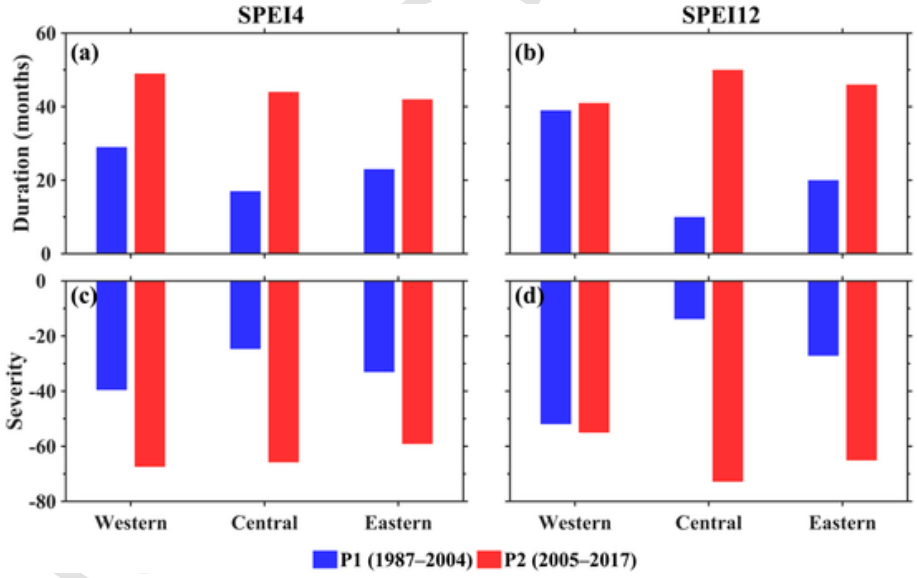

Fig. 5. (a, b) Total duration and (c, d) total severity for SPEI4 and SPEI12 over the Western, Central, and Eastern regions during the P1 period (1987–2004) and P2 period (2005–2017).

ally, along with its variability is a significant concern, as Nepal's agriculture mainly relies on monsoonal precipitation. Moreover, based on section 1, the summer drought characteristic change and telecommunication with atmospheric circulation is the recent need of Nepal. Therefore, we examined the temporal evolution of SPEI4 in September (SPEI4-Sep) that is considered the summer drought index in Fig. 6(a-c). During the study period, the total number of summer drought events ranged between 5 and 8 in all three regions. In the Western region, eight years (1992, 1994, 2002, 2004, 2005, 2006, 2012, and 2015) experienced summer drought, mainly increased after the 2000s (Fig. 6a). Further, consecutive summer droughts were observed in the Western region during 2001–2007. A total of five (1992, 2005, 2006, 2009, and 2015) and six (1992, 1994, 2009, 2012, 2013, and 2015) summer drought years were observed in the Central and Eastern regions, respectively (Fig. 6b and c). The severe summer drought (SPEI ≤ -1.5) was experienced during 1992 in Western and Eastern, 2006 in Central, 2009 in Eastern, and 2015 in Western and Central regions. During the P1 period, the Central and Eastern regions did not experience prolonged drought, whereas these regions suffered more extended drought during the P2 period. In addition, the total severity has increased from −2.5 to

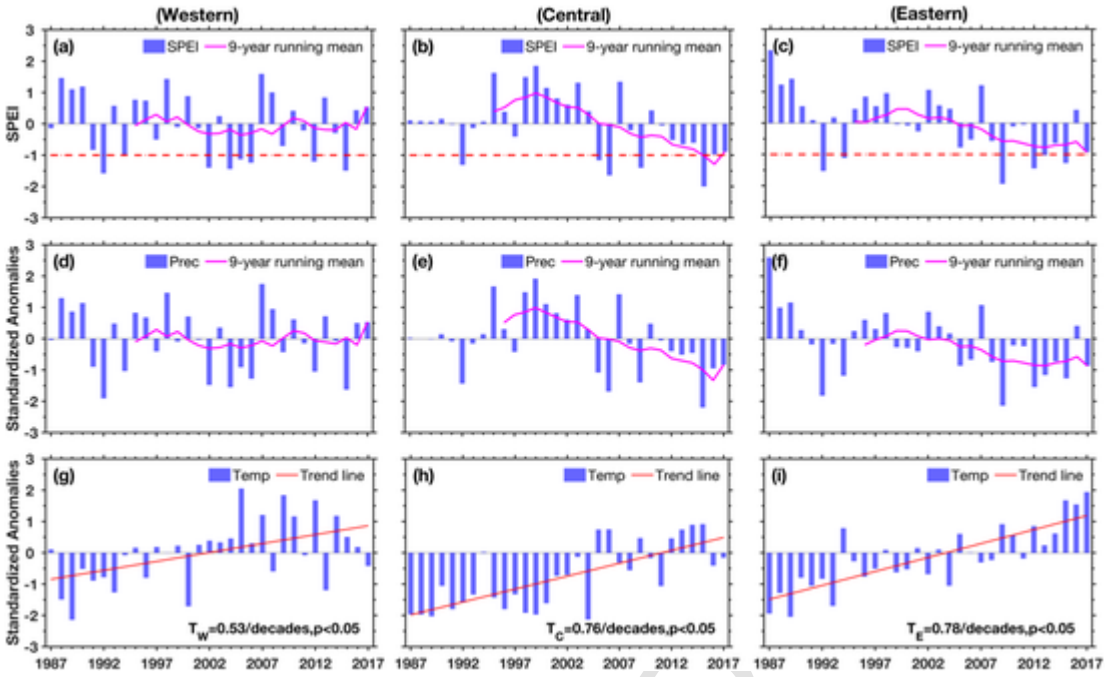

Fig. 6. Temporal variation of (a, b, c) summer drought index (SPEI4-Sep), (d, e, f) precipitation, and (g, h, i) mean temperature for Western, Central, and Eastern regions during 1987–2017. The red dash line represents the threshold level (−1) of drought. The magenta and red line indicates a 9-year running average and linear trend. (For interpretation of the references to colour in this figure legend, the reader is referred to the web version of this article.)

−5.1 in Central whereas from −2.6 to −6.2 in the Eastern region. Meanwhile, summer drought events increased five times in the Central region, two times in the Eastern region, and remained the same in the Western region after 2004. A significant decadal shift from wet to dry conditions in the Central and Eastern regions can be observed from the 9-year running mean of SPEI4-Sep (Fig. 6b and c). However, the dominant feature of summer drought variation in the Western region shows the interannual variability (Fig. 6a).

The low precipitation initiates the summer drought condition (Ahmed et al., 2018), while increased temperature further enhances drought severity and intensity (Amrit et al., 2018). To understand the variation of summer drought over different regions, we analyzed the temporal variation of summer precipitation and temperature anomalies in Fig. 6(d-i). The average total precipitation in the Western region during the summer monsoon is 1455 mm, while precipitation is higher in the Central and Eastern regions, with 1787 mm and 1587 mm. The interannual precipitation change for the Western region is elucidated in Fig. 6d, with consecutive negative precipitation anomalies between 2000 and 2007. On the other hand, the remarkable interdecadal change of summer precipitation was observed in the Central and Eastern regions, with more negative (positive) precipitation anomalies in the Central and Eastern region after (before) 2004 (Fig. 6e and f).

The average temperature in all three regions shows a consistently increasing trend from 1987 to 2017 at a 95% confidence level (Fig. 6g-i). The average increasing temperature rate is 0.53 °C/decade, 0.76 °C/decade, and 0.78 °C/decade in the Western, Central, and Eastern regions. This reveals that the temperature has been continuously increasing in all three regions; however, positive temperature anomalies were observed during the P2 period. The increased temperature and decreased summer precipitation enhanced the drought duration and severity over the Central and Eastern regions. In contrast, the Western region did not experience significant precipitation change that reflects no change in drought frequency from P1 to P2 periods, even though the Western region has experienced more drought events altogether than the other two regions (Table 2).

3.5. Associated atmospheric circulation for summer drought variation

The summer drought phase is similar to the summer precipitation variation over different regions of Nepal (Fig. 6). Therefore, we analyzed the spatial distribution of summer precipitation over the South Asian monsoon region using ERA5 reanalysis datasets (Fig. 7). The highest precipitation has occurred in the Western Ghats of India and Southeast Asia (Fig. 7a). The amount of precipitation during the monsoon spatially varies from 800 to 3000 mm from west to east Nepal (Fig. 7a). The Central (2580 mm) and Eastern regions (2272 mm) are relatively wetter than the Western (2053 mm) regions. The whole period climatology of precipitation subtracted from the P1 and P2 period's climatology is presented in Figs. 7b and c. For the P1 period, positive anomalies can be found over the Indian Peninsula and Bay of Bengal (BoB); moreover, the Central and Eastern region also has positive anomalies (Fig. 7b). The Western region does not show significant precipitation anomalies in both periods. However, the precipitation anomalies in the P2 period are the opposite of the P1 period in the Central and Eastern region (Fig. 7b), indicating the precipitation weakening during the P2 period. Moreover, negative anomalies are observed over the Arabian Sea (AS), Indian peninsula, and the Bay of Bengal. It also reveals the strengthening of the SASM during the P1 period and weakening during the P2 period (Fig. 7b and c).

Further, we conducted the correlation between the SASM index (5°-22.5°N, 35°-97.5°E) and summer drought index of Nepal regions in Table 3. It shows that the variation of summer drought over the Central and Eastern is significantly positively correlated with the variation of the SASM. The correlation is positive in the Western region; however, not significant. The result indicates that the interdecadal enhancement of drought in the Central and Eastern region is coherent with the interdecadal shift of the SASM after 2004 (can be viewed in http://ljp.gcess.cn/dct/page/65576).

To understand large-scale atmospheric circulation patterns responsible for the interannual variation of summer drought in the Western region, whereas decadal variation in the Central and Eastern regions, the climatology of wind at 850 hPa during 1987–2017, and anomalies for P1 and P2 periods are shown in Fig. 8. The winds at low-level (850 hPa)

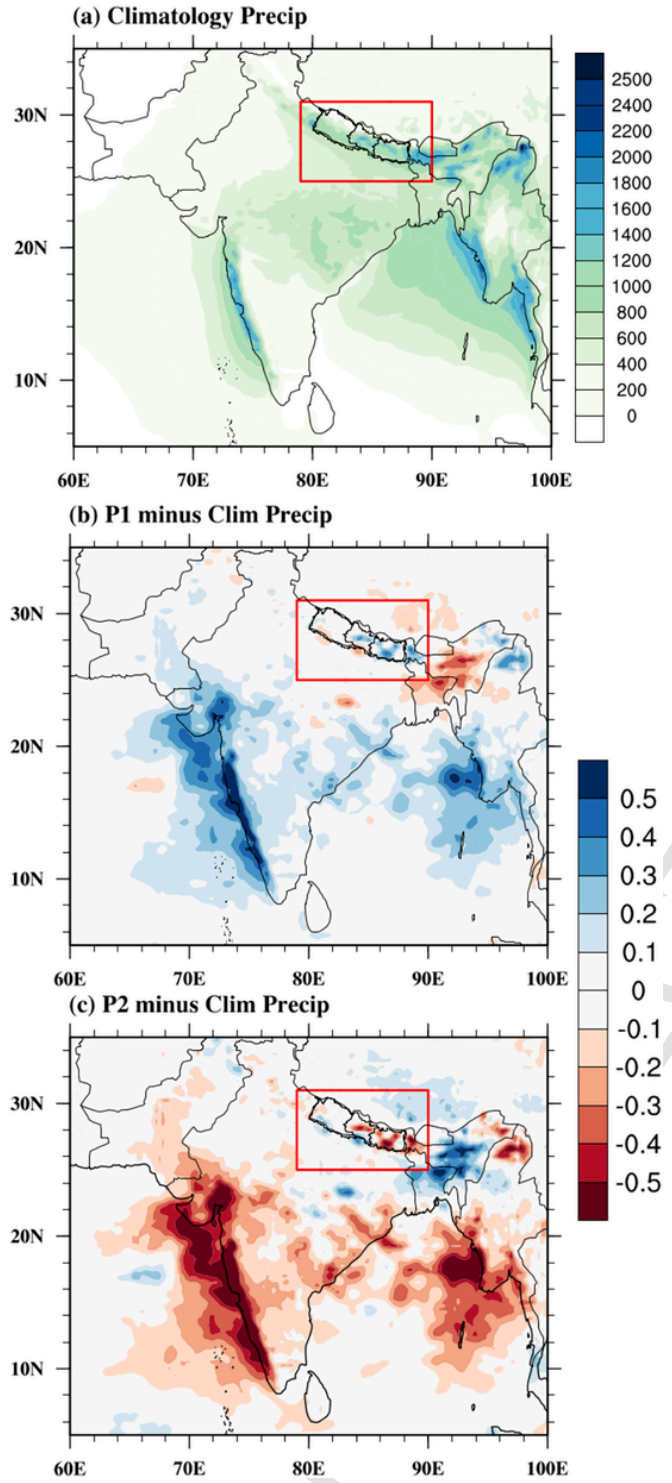

Fig. 7. (a) The climatology of the summer precipitation (mm) averaged over 1987–2017. Precipitation anomalies for (b) P1 period (1987–2004), and (c) P2 period (2005–2017) from the long-term climatology (1987–2017). The red box shows the study area. (For interpretation of the references to colour in this figure legend, the reader is referred to the web version of this article.)

are characterized by the strongest westerlies over the Arabian Sea during the summer monsoon season (Goswami, 2005; Sharma et al., 2020b). Fig. 8a shows that low-level wind circulation has strengthened westerly cross-equatorial monsoonal flow associated with enhanced precipitation over the South Asian region, and the monsoon trough (low-pressure system) is located around the south of Central Himalaya.

Table 3
Correlation between SASM index and summer drought index (SPEI4-Sep).

Region	Correlation
Western	0.18
Central	0.37*
Eastern	0.30*

* Represents the significance at 90% confidence interval.

As a result, the warm and humid air masses from the AS and BoB enter the Eastern and Central region and advances westward. During the P1 period, the wind circulation was relatively stronger, with enhanced wind anomalies (westerlies) and the strengthened cross-equatorial flow (Fig. 8b). Moreover, the cyclonic circulation was formed over the Indo-Gangetic plain below the Central and Eastern regions, whereas anti-cyclonic circulation over BoB. The result indicates that the enormous moisture is transported from the AS and BoB to the Indo-Gangetic plain and eastern part of Central Himalaya. Further, the strengthened wind anomalies were observed over the Eastern and Central regions compared to the Western region. However, the low-level wind circulation was relatively weaker in the P2 period with weaker wind anomalies (easterlies) and cross-equatorial flow (Fig. 8c). As a result, it formed anti-cyclonic circulation over the Indo-Gangetic plain below the Central and Eastern regions, whereas cyclonic circulation over BoB. This system reduced water vapour transportation from the south (i.e., AS and BoB) to the north (i.e., mainly over the eastern half of Nepal), thus, induces less precipitation with frequent and intensified drought episodes in that region.

The mean moisture flux divergence has intensified from the 21st century, which counters the drying caused by the enhanced mean moisture flux divergence (Gao et al., 2012). We further analyzed the Vertically Integrated Divergence Moisture Flux (VIDMF) for the summer season from 1987 to 2017 (Fig. 9). It is observed that VIMDF is negative over the BoB region, suggesting a high sink of the moisture convergence (negative anomalies) at a magnitude of 15 $\times$ 10^{-5} Kg m^{-2} s^{-1}. It also revealed a higher moisture flux convergence in the Central (12.5 $\times$ 10^{-5} Kg m^{-2} s^{-1}) and Eastern (9.2 $\times$ 10^{-5} Kg m^{-2} s^{-1}) regions than the Western region (3.46 $\times$ 10^{-5} Kg m^{-2} s^{-1}) during the study period (Fig. 9a). The long-term mean of VIMDF shows 3 to 4 times less moisture convergence in the Western region than the Eastern and Central regions, which can be the reason for the interannual variation of the drought episodes (Fig. 9a). During the P1 period, there were negative anomalies (moisture convergence) widespread in Central, Eastern and Far-western regions, suggesting more water vapour transport in the region from the Ocean (Fig. 9b). However, positive anomalies (moisture divergence) were observed during the P2 period weakened the water vapour transport mainly over the Eastern and Central regions (Fig. 9c). Meanwhile, the Western region shows convergence and divergence patterns during the study period (P1 and P2) consistent with precipitation climatology (Figs. 7c and 9c). The result indicates that less moisture is driven from Ocean (AS and BoB) to the study area during the P2 period. Moreover, the interdecadal differences of moisture divergence in the Central and Eastern region subsequently explain the weakening of the precipitation in the P2 period, hence inducing enhanced drought episodes.

4. Discussion

The spatiotemporal variation of drought characteristics across Nepal has been investigated using the SPEI considering both temperature and precipitation from 1987 to 2017, while most of the earlier studies have considered only precipitation (SPI method) to study drought (Dahal et al., 2015; Kafle, 2015; Sigdel and Ikeda, 2010). Three different regions (Western, Central, and Eastern) of Nepal have experienced a remarkable drought variation and strengthening of drought after 2004. Meanwhile, the cumulative probability of short-term (long-term) drought for the Western, Central, and Eastern regions has in-

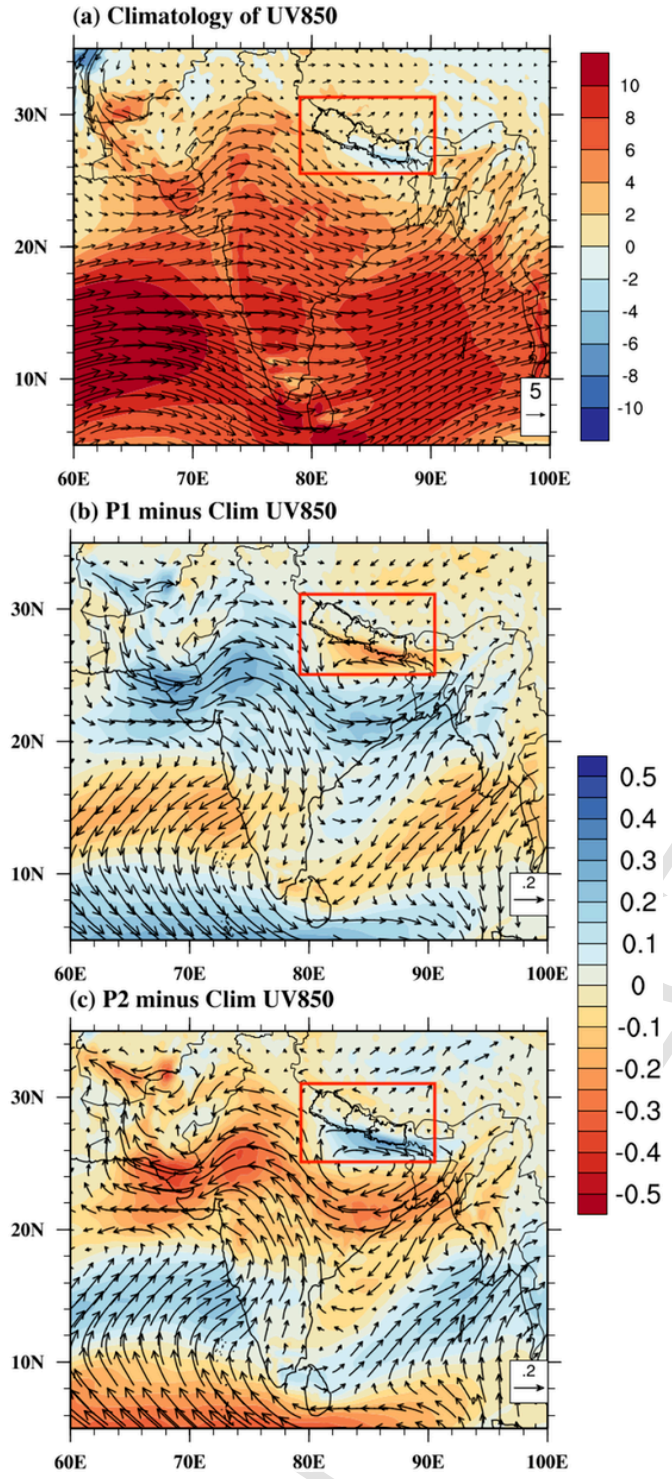

Fig. 8. (a) The climatology of the summer wind at 850 hPa (m/s, shading: u-component of wind) averaged over 1987–2017. Wind anomalies for (b) P1 period (1987–2004) and (c) P2 period (2005–2017) from the long-term climatology (1987–2017). The red box shows the study area. (For interpretation of the references to colour in this figure legend, the reader is referred to the web version of this article.)

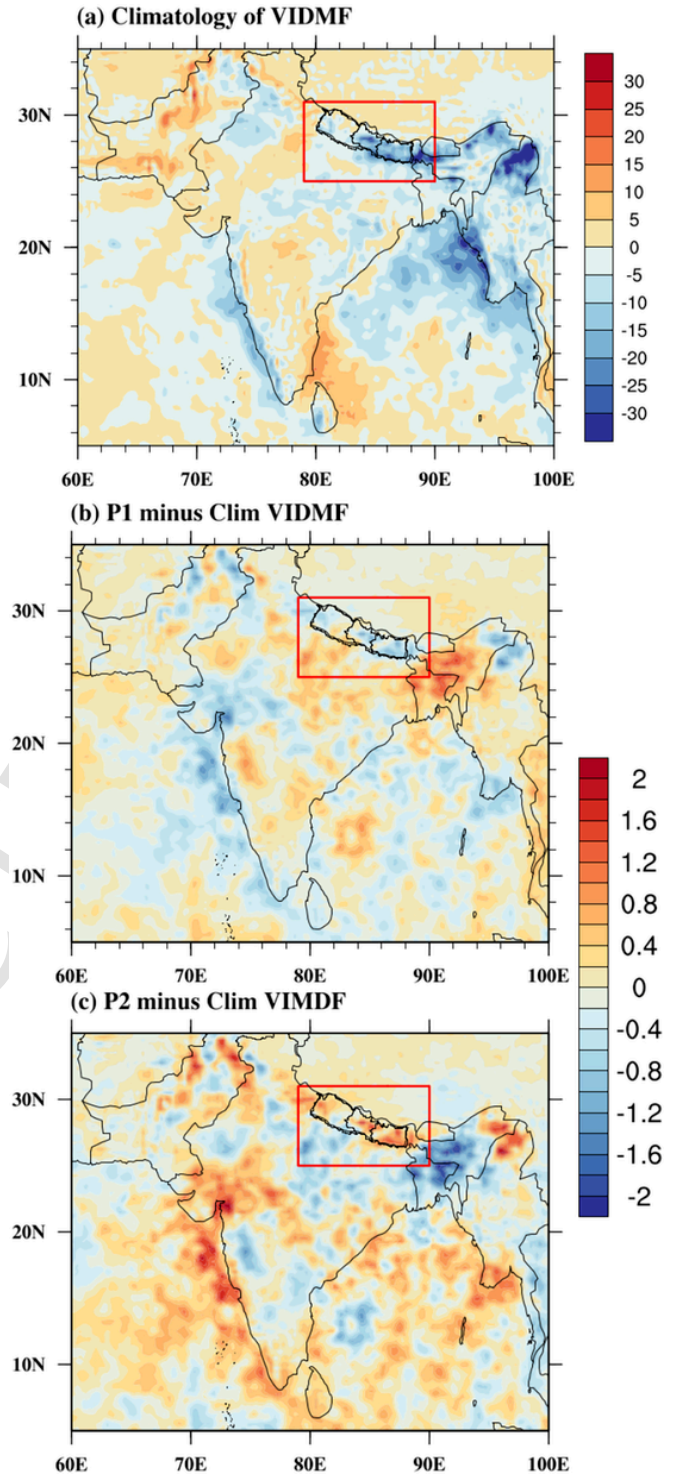

Fig. 9. (a) Vertically Integrated Divergence Moisture flux (VIDMF, 10^{-5} Kg m^{-2} s^{-1}; negative and positive values indicate moisture convergence and divergence, respectively), averaged over 1987–2017. VIMDF anomalies for (b) P1 period (1987–2004) and (c) P2 period (2005–2017) from the long-term climatology (1987–2017). The red box shows the study area. (For interpretation of the references to colour in this figure legend, the reader is referred to the web version of this article.)

creased by 15 (2) %, 18 (31) %, and 15 (15) %, respectively, from P1 (1987–2004) to P2 (2005–2017) periods. Moreover, drought frequency, duration, and severity drastically increased in the P2 period suggesting the interdecadal enhancement of drought characteristics, mainly in the Central and Eastern regions. For instance, in the Central region, the total duration (severity) was 10 (−13.8) during the P1 period, which later increased to 50 (−72.8) in the P2 period at a long-term timescale.

The 9-year running average of summer drought showed the interannual variability in the Western region, whereas decadal variability in the Central and Eastern regions. This is the case of regional variation of

summer precipitation, as previous studies have shown the east-west division of precipitation with a high amount in the Central and Eastern regions than in the Western region (Kansakar et al., 2004; Pokharel et al., 2019; Sharma et al., 2020a). Moreover, the Western region has less moisture convergence and is relatively drier than other regions, so the drought variation has remained the same throughout the period. In contrast, the decadal variation of drought in the Central and Eastern regions is consistent with decadal precipitation changes in the South Asian region (Mallya et al., 2016; Kumar et al., 2013). Further, Ma et al. (2019) also reported the interdecadal change in the South Asian Monsoon after 2000. Meanwhile, Hernandez et al. (2015) showed an increase in drought characteristics such as frequency, severity, and intensity in recent decades, as the South Asian monsoon is getting drier.

The interdecadal variation of summer drought in Nepal was attributed to the changing phase of the summer precipitation. Moreover, the decadal weakening of the SASM is the key reason for enhancing the drought in the Central and Eastern regions of Nepal. The decadal variation of SASM was due to changes in the Walker and Hadley circulation that influence the low-level wind circulation, altering the moisture supply to the Indian sub-continent (Hrudya et al., 2020). Our study verifies summer drought variation through precipitation, wind circulation, and moisture flux convergence/divergence. The interdecadal weakening of the monsoon was characterized by weakening wind anomalies with anti-cyclonic circulation and moisture divergence over the Indo-Gangetic plain and Nepal, respectively. The result is consistent with Hernandez et al. (2015), which found dry northerly wind over the Indo-Gangetic plain with drying signals at decadal timescales. Similarly, Roxy et al. (2015) reported the reduced precipitation over the Indian subcontinent due to weakened mean south-westerly winds. Further, anti-cyclonic circulation over the Indo-Gangetic plain suppressed moisture supplements from the nearby Ocean (Ge et al., 2017; Singh et al., 2014). The AS and BoB are moisture transport sources to the South Asian region and Nepal during the summer (Chen et al., 2021; Sharma et al., 2020b). The low-pressure systems are observed over the BoB, propagating along the monsoon core zone, contributing to significant precipitation (Gadgil et al., 2003; Hrudya et al., 2020). During the P2 period, relatively less moisture was transported from the southern BoB, and the moisture divergence dominates Nepal, resulting in increased drought episodes. Moreover, the recent study of Maharana et al. (2021) showed that moisture transport has weakened over the Indo-Gangetic plains and northeast India during the recent warming period (2001–2018), leading to a decline in the summer precipitation with increasing dryness.

The role of the Sea Surface Temperature (SST) anomalies in the interannual and decadal variability of the summer monsoon have also been studied (Kumar et al., 2013; Sharma et al., 2020b; Sun et al., 2019). The recent study observed a below-normal precipitation pattern (dryness) at an interannual timescale over Nepal due to the El Niño summer, which disturbed the wind circulation, relative humidity, and monsoon trough (Sharma et al., 2020b). Further, they also described the mechanism of the dryness pattern in summer over Eastern Nepal, which is associated with interannual basin-wide cooling of the tropical Indian Ocean. On the other hand, the warm SST anomalies over the Pacific Ocean disturbed the monsoon circulation by delaying the monsoon precipitation and causing the precipitation deficit in South Asian countries (Joshi and Kar, 2018; Mishra et al., 2016; Sharma et al., 2020b). Further, the decadal variation of SASM is related to the warm phase of Pacific Decadal Oscillation (PDO), as already described by previous studies (Krishnamurthy and Krishnamurthy, 2014; Watanabe and Yamazaki, 2014). Therefore, future studies should focus on the SST signals for interdecadal drought characteristics in Nepal. Overall, this study mainly focused on the variation of drought characteristics due to precipitation change over Nepal. However, long-term temperature trends on drought have not been investigated in Nepal, as other studies show increasing temperature can amplify drought severity and intensity (Amrit et al., 2018; Beguería et al., 2014; Vicente-Serrano et al., 2010; Yao et al., 2016). In particular, increasing temperature and its impact on drought need to be further studied. Furthermore, we recommend comparing different PET computation methods with the availability of reliable long-term data, such as from synoptic weather stations at Kathmandu and other places of Nepal.

5. Conclusion

In this study, drought characteristics were investigated using SPEI, utilizing the observed monthly precipitation and temperature datasets over the Western, Central, and Eastern regions of Nepal during 1987–2017 at short-term (SPEI4) and long-term (SPEI12) timescale. The severe drought years were observed in 1992, 1994, 2006, 2008, 2009, 2012, 2015, and 2016. The different regions (Western, Central, and eastern) have experienced a remarkable variation and strengthening of drought characteristics after 2004. The cumulative occurrences of SPEI4 drought in the Western, Central, and Eastern regions have increased by 15%, 18%, and 15%, respectively, from P1(1987–2004) to P2(2005–2017) periods. Additionally, SPEI12 showed an increased drought frequency by 2%, 31%, and 16% in Western, Central, and Eastern regions, respectively, from P1 to P2 periods. At a short-term timescale, the total drought duration and severity in the P2 period were almost twice the P1 period in all three regions. The duration and severity are almost equal in the Western region; however, they are 5 and 2.4 folds longer and severe in the Central and Eastern regions at the long-term timescale.

Further, we analyzed drought change and the associated atmospheric circulation for summer drought (SPEI4-Sep) variation over three regions of Nepal. The summer drought events increased five times in the Central region, two times in the Eastern Region, and did not observe any change in the Western region after 2004. The result indicates the interannual variation in Western Nepal, whereas decadal variation was predominant in the Central and Eastern regions. The variation of summer drought in Nepal was attributed to the changing phase of the summer precipitation. The large-scale atmospheric circulations revealed the negative summer precipitation anomalies due to weakening wind anomalies with anti-cyclonic circulation and moisture divergence over the Indo-Gangetic plain and Nepal, respectively, with more drought episodes after 2004. Furthermore, the moisture transport from the AS and BoB to the study region is weaker, resulting in more drought events, especially in the Central and Eastern regions. These increased drought episodes might influence the agriculture and water resources over the Central and Eastern regions in recent years. Therefore, it guides relevant stakeholders to make effective mitigation and adaptation plans; and reduce future drought risks.

Author contribution

K. Hamal had the original idea and drafted the paper with help from N. Khadka and S. Sharma. All authors participated in the discussion, reviewed, and improved the manuscript.

Funding

This research did not receive any specific grant from funding agencies in the public, commercial, or not-for-profit sectors.

Data availability statement

The ERA5 data sets used in this study were developed and maintained by European Centre for Medium-Range Weather Forecasts, which can be freely accessed from https://cds.climate.copernicus.eu/cdsapp#!/dataset/reanalysis-era5-pressure-levels-monthly-means?tab=form. The daily datasets for all the stations used in this

study can be purchased online from DHM, Government of Nepal (http://www.dhm.gov.np/).

Uncited references

Sharma et al., 2020c

CRediT authorship contribution statement

Kalpana Hamal: Conceptualization, Methodology, Software, Investigation, Writing – original draft. **Shankar Sharma:** Conceptualization, Visualization, Writing – review & editing. **Binod Pokharel:** Supervision, Writing – review & editing. **Dibas Shrestha:** Writing – review & editing. **Rocky Talchabhadel:** Writing – review & editing. **Alen Shrestha:** Writing – review & editing. **Nitesh Khadka:** Conceptualization, Investigation, Writing – review & editing.

Declaration of Competing Interest

The authors declare that they have no known competing financial interests or personal relationships that could have appeared to influence the work reported in this paper.

Acknowledgment

The authors would like to express their sincere gratitude to the Department of Hydrology and Meteorology (DHM), Nepal, to provide station datasets and Scientists at European Centre for Medium–Range Weather Forecasts (ECMWF) to provide ERA5 datasets. K. Hamal is supported by the ANSO young talents fellowship, and N. Khadka is supported by the CAS-TWAS President's fellowship. The authors also thankful to anonymous reviewers for their insightful comments and suggestions, which helped to improve the manuscript.

References

Aadhar, S., Mishra, V., 2017. High-resolution near real-time drought monitoring in South Asia. Sci Data. 4, 170145. https://doi.org/10.1038/sdata.2017.145.

Ahmed, K., Shahid, S., Nawaz, N., 2018. Impacts of climate variability and change on seasonal drought characteristics of Pakistan. Atmos. Res. 214, 364–374. https://doi.org/10.1016/j.atmosres.2018.08.020.

Allen, R., Pereira, L., Raes, D., Smith, M., 1998. Crop evapotranspiration: Guidelines for computing crop water requirements. In: FAO Irrigation and Drainage Paper (56), 300 Pp FAO, Rome, Italy.

Amrit, K., Pandey, R.P., Mishra, S.K., Daradur, M., 2018. Relationship of drought frequency and severity with range of annual temperature variation. Nat. Hazards 92, 1199–1210.

Baniya, B., Tang, Q., Xu, X., Haile, G.G., Chhipi-Shrestha, G., 2019. Spatial and temporal variation of drought based on satellite derived vegetation condition index in Nepal from 1982–2015. Sensors. 19, 430.

Beguería, S., Vicente-Serrano, S.M., Reig, F., Latorre, B., 2014. Standardized precipitation evapotranspiration index (SPEI) revisited: parameter fitting, evapotranspiration models, tools, datasets and drought monitoring. Int. J. Climatol. 34, 3001–3023.

C3S, 2017. Copernicus Climate Change Service: ERA5: Fifth generation of ECMWF atmospheric reanalyses of the global climate. In: Copernicus Climate Change Service Climate Data Store (CDS), November, 2019. https://cds.climate.copernicus.eu/cdsapp#!/home.

Chen, Y., Sharma, S., Zhou, X., Yang, K., Li, X., Niu, X., Hu, X., Khadka, N., 2021. Spatial performance of multiple reanalysis precipitation datasets on the southern slope of central Himalaya. Atmos. Res. 250, 105365. https://doi.org/10.1016/j.atmosres.2020.105365.

Dahal, P., Shrestha, N.S., Shrestha, M.L., Krakauer, N.Y., Panthi, J., Pradhanang, S.M., Jha, A., Lakhankar, T., 2015. Drought risk assessment in Central Nepal: temporal and spatial analysis. Nat. Hazards 80, 1913–1932. https://doi.org/10.1007/s11069-015-2055-5.

Fahad, S., Bajwa, A.A., Nazir, U., Anjum, S.A., Farooq, A., Zohaib, A., Sadia, S., Nasim, W., Adkins, S., Saud, S., Ihsan, M.Z., Alharby, H., Wu, C., Wang, D., Huang, J., 2017. Crop production under drought and heat stress: plant responses and management options. Front. Plant Sci. 8, 1147. https://doi.org/10.3389/fpls.2017.01147.

Feba, F., Ashok, K., Ravichandran, M., 2019. Role of changed Indo-Pacific atmospheric circulation in the recent disconnect between the Indian summer monsoon and ENSO. Clim. Dyn. 52, 1461–1470.

Gadgil, S., Vinayachandran, P., Francis, P., 2003. Droughts of the Indian summer monsoon: Role of clouds over the Indian Ocean. Curr. Sci. 1713–1719.

Gao, Y., Leung, L.R., Salathé, Jr., E.P., Dominguez, F., Nijssen, B., Lettenmaier, D.P., 2012. Moisture flux convergence in regional and global climate models: Implications for droughts in the southwestern United States under climate change. Geophys. Res. Lett. 39.

Ge, F., Sielmann, F., Zhu, X., Fraedrich, K., Zhi, X., Peng, T., Wang, L., 2017. The link between Tibetan Plateau monsoon and Indian summer precipitation: a linear diagnostic perspective. Clim. Dyn. 49, 4201–4215. https://doi.org/10.1007/s00382-017-3585-1.

Goswami, B., 2005. South Asian monsoon. In: Intraseasonal Variability in the Atmosphere-Ocean Climate System. Springer, pp. 19–61.

Guo, Y., Huang, S., Huang, Q., Wang, H., Fang, W., Yang, Y., Wang, L., 2019. Assessing socioeconomic drought based on an improved Multivariate standardized Reliability and Resilience Index. J. Hydrol. 568, 904–918.

Gyawali, S., 2016. In West Nepal, a River Basin Is a Home to Drought and Poverty. (Lack of data prevents a planned response to climate change in the Karnali river basin).

Haile, G.G., Tang, Q., Li, W., Liu, X., Zhang, X., 2020. Drought: Progress in broadening its understanding. Wiley Interdiscip. Rev. Water 7, e1407.

Hamal, K., Sharma, S., Baniya, B., Khadka, N., Zhou, X., 2020a. Inter-Annual variability of winter precipitation over Nepal coupled with ocean-atmospheric patterns during 1987–2015. Front. Earth Sci. 8, 161. https://doi.org/10.3389/feart.2020.00161.

Hamal, K., Sharma, S., Khadka, N., Baniya, B., Ali, M., Shrestha, M.S., Xu, T., Shrestha, D., Dawadi, B., 2020b. Evaluation of MERRA-2 precipitation products using gauge observation in Nepal. Hydrology. 7, 40. https://doi.org/10.3390/hydrology7030040.

Hamal, K., Sharma, S., Khadka, N., Haile, G.G., Joshi, B.B., Xu, T., Dawadi, B., 2020c. Assessment of drought impacts on crop yields across Nepal during 1987–2017. Meteorol. Appl. 27, e1950.

Hernandez, M., Ummenhofer, C.C., Anchukaitis, K.J., 2015. Multi-scale drought and ocean–atmosphere variability in monsoon Asia. Environ. Res. Lett. 10, 074010.

Herrera-Estrada, J.E., Satoh, Y., Sheffield, J., 2017. Spatiotemporal dynamics of global drought. Geophys. Res. Lett. 44, 2254–2263.

Hrudya, P., Varikoden, H., Vishnu, R., 2020. A review on the Indian summer monsoon rainfall, variability and its association with ENSO and IOD. Meteorog. Atmos. Phys. 1–14.

Jin, Q., Wang, C., 2017. A revival of Indian summer monsoon rainfall since 2002. Nat. Clim. Chang. 7, 587–594.

Joshi, S., Kar, S.C., 2018. Mechanism of ENSO influence on the south Asian monsoon rainfall in global model simulations. Theor. Appl. Climatol. 131, 1449–1464.

Kafle, H.K., 2015. Spatial and Temporal Variation of Drought in Far and Mid Western Regions of Nepal: Time Series Analysis (1982-2012). Nepal J. Sci. Technol. 15, 65–76. https://doi.org/10.3126/njst.v15i2.12118.

Kansakar, S.R., Hannah, D.M., Gerrard, J., Rees, G., 2004. Spatial pattern in the precipitation regime of Nepal. Int. J. Climatol. 24, 1645–1659. https://doi.org/10.1002/joc.1098.

Karki, R., Schickhoff, U., Scholten, T., Böhner, J., 2017. Rising precipitation extremes across Nepal. Climate. 5, 4.

Khatiwada, K.R., Pandey, V.P., 2019. Characterization of hydro-meteorological drought in Nepal Himalaya: a case of Karnali River Basin. Weather Clim. Extrem. 26, 100239. https://doi.org/10.1016/j.wace.2019.100239.

Krishnamurthy, L., Krishnamurthy, V., 2014. Decadal scale oscillations and trend in the Indian monsoon rainfall. Clim. Dyn. 43, 319–331.

Krishnamurthy, V., Shukla, J., 2000. Intraseasonal and interannual variability of rainfall over India. J. Clim. 13, 4366–4377.

Kumar, K.N., Rajeevan, M., Pai, D., Srivastava, A., Preethi, B., 2013. On the observed variability of monsoon droughts over India. Weather Clim. Extrem. 1, 42–50. https://doi.org/10.1016/j.wace.2013.07.006.

Liu, X., Zhu, X., Pan, Y., Bai, J., Li, S., 2018. Performance of different drought indices for agriculture drought in the North China Plain. J. Arid Land. 10, 507–516. https://doi.org/10.1007/s40333-018-0005-2.

Ma, H., Zhu, Y., Hua, W., 2019. Interdecadal change in the south Asian summer monsoon rainfall in 2000 and contributions from regional tropical SST. Atmos. Oceanic Sci. Lett. 12, 399–408. https://doi.org/10.1080/16742834.2019.1648168.

Maharana, P., Agnihotri, R., Dimri, A.P., 2021. Changing Indian monsoon rainfall patterns under the recent warming period 2001–2018. Clim. Dyn.. https://doi.org/10.1007/s00382-021-05823-8.

Mallya, G., Mishra, V., Niyogi, D., Tripathi, S., Govindaraju, R.S., 2016. Trends and variability of droughts over the Indian monsoon region. Weather Clim. Extrem. 12, 43–68.

Mavromatis, T., 2007. Drought index evaluation for assessing future wheat production in Greece. Int. J. Climatol. 27, 911–924.

McKee, T.B., Doesken, N.J., Kleist, J., 1993. The relationship of drought frequency and duration to time scales. In: Proceedings of the 8th Conference on Applied Climatology, Boston. pp. 179–183.

Mishra, A.K., Singh, V.P., 2010. A review of drought concepts. J. Hydrol. 391, 202–216. https://doi.org/10.1016/j.jhydrol.2010.07.012.

Mishra, V., Aadhar, S., Asoka, A., Pai, S., Kumar, R., 2016. On the frequency of the 2015 monsoon season drought in the Indo-Gangetic Plain. Geophys. Res. Lett. 43 (12), 102–112,112.

Miyan, M.A., 2015. Droughts in Asian Least developed Countries: Vulnerability and sustainability. Weather Clim. Extrem. 7, 8–23. https://doi.org/10.1016/j.wace.2014.06.003.

MoFE, 2019. Climate change scenarios for Nepal for National Adaptation Plan (NAP). 1. Ministry of Forests and Environment, Kathmandu, Nepal, p. 74.

Omidvar, K., Fatemi, M., Narangifard, M., Hatami Bahman Beiglou, K., 2016. A Study of the Circulation patterns Affecting Drought and Wet Years in Central Iran. Adv. Meteorol. 2016.

Palmer, W.C., 1965. Meteorological Drought. US Department of Commerce, Weather Bureau.

Panthi, S., Bräuning, A., Zhou, Z.-K., Fan, Z.-X., 2017. Tree rings reveal recent intensified

spring drought in the central Himalaya, Nepal. Glob. Planet. Chang. 157, 26–34. https://doi.org/10.1016/j.gloplacha.2017.08.012.
Pokharel, B., Wang, S.Y.S., Meyer, J., Marahatta, S., Nepal, B., Chikamoto, Y., Gillies, R., 2019. The east–west division of changing precipitation in Nepal. Int. J. Climatol. 40, 3348–3359. https://doi.org/10.1002/joc.6401.
Portela, M.M., Santos, J., de Carvalho Studart, T.M., 2019. Effect of the Evapotranspiration of Thornthwaite and of Penman-Monteith in the Estimation of Monthly Streamflows Based on a Monthly Water Balance Model. Current Practice in Fluvial Geomorphology-Dynamics and Diversity. IntechOpen.
Reichstein, M., Bahn, M., Ciais, P., Frank, D., Mahecha, M.D., Seneviratne, S.I., Zscheischler, J., Beer, C., Buchmann, N., Frank, D.C., 2013. Climate extremes and the carbon cycle. Nature. 500, 287.
Roxy, M.K., Ritika, K., Terray, P., Murtugudde, R., Ashok, K., Goswami, B.N., 2015. Drying of Indian subcontinent by rapid Indian Ocean warming and a weakening land-sea thermal gradient. Nat. Commun. 6, 7423. https://doi.org/10.1038/ncomms8423.
Sharma, S., Chen, Y., Zhou, X., Yang, K., Li, X., Niu, X., Hu, X., Khadka, N., 2020a. Evaluation of GPM-Era Satellite Precipitation Products on the Southern Slopes of the Central Himalayas against rain Gauge Data. Remote Sens. 12, 1836. https://doi.org/10.3390/rs12111836.
Sharma, S., Hamal, K., Khadka, N., Joshi, B.B., 2020b. Dominant pattern of year-to-year variability of summer precipitation in Nepal during 1987–2015. Theor. Appl. Climatol. 142, 1071–1084. https://doi.org/10.1007/s00704-020-03359-1.
Sharma, S., Khadka, N., Hamal, K., Baniya, B., Luintel, N., Joshi, B.B., 2020c. Spatial and Temporal analysis of precipitation and its extremities in seven provinces of Nepal (2001-2016). Appl. Ecol. Environ. Sci. 8, 64–73. https://doi.org/10.12691/aees-8-2-4.
Sharma, S., Khadka, N., Hamal, K., Shrestha, D., Talchabhadel, R., Chen, Y., 2020d. How accurately can satellite products (TMPA and IMERG) detect precipitation patterns extremities, and drought across the Nepalese Himalaya?. Earth Space Sci. 7 e2020EA001315 https://doi.org/10.1029/2020ea001315.
Sharma, S., Hamal, K., Khadka, N., Shrestha, D., Aryal, D., Thakuri, S., 2021a. Drought characteristics over Nepal Himalaya and their relationship with climatic indices. Meteorol. Appl. 28, e1988.
Sharma, S., Khadka, N., Nepal, B., Ghimire, S.K., Luintel, N., Hamal, K., 2021b. Elevation Dependency of Precipitation over Southern Slope of Central Himalaya. Jalawaayu. 1, 1–14.
Shen, Z., Zhang, Q., Singh, V.P., Sun, P., Song, C., Yu, H., 2019. Agricultural drought monitoring across Inner Mongolia, China: Model development, spatiotemporal patterns and impacts. J. Hydrol. 571, 793–804. https://doi.org/10.1016/j.jhydrol.2019.02.028.
Shrestha, A., Rahaman, M.M., Kalra, A., Jogineedi, R., Maheshwari, P., 2020a. Climatological drought forecasting using bias corrected CMIP6 climate data: a case study for India. Forecasting. 2, 59–84.
Shrestha, A., Rahaman, M.M., Kalra, A., Thakur, B., Lamb, K.W., Maheshwari, P., 2020b. Regional Climatological Drought: an Assessment using High-Resolution Data. Hydrology. 7, 33.
Sigdel, M., Ikeda, M., 2010. Spatial and temporal analysis of drought in Nepal using standardized precipitation index and its relationship with climate indices. J. Hydrol. Meteorol. 7, 59–74.
Singh, D., Tsiang, M., Rajaratnam, B., Diffenbaugh, N.S., 2014. Observed changes in extreme wet and dry spells during the south Asian summer monsoon season. Nat. Clim. Chang. 4, 456.
Sun, B., Li, H., Zhou, B., 2019. Interdecadal variation of Indian Ocean basin mode and the impact on Asian summer climate. Geophys. Res. Lett. 46, 12388–12397. https://doi.org/10.1029/2019gl085019.
Talchabhadel, R., Karki, R., Thapa, B.R., Maharjan, M., Parajuli, B., 2018. Spatio-temporal variability of extreme precipitation in Nepal. Int. J. Climatol. 38, 4296–4313. https://doi.org/10.1002/joc.5669.
Talchabhadel, R., Karki, R., Yadav, M., Maharjan, M., Aryal, A., Thapa, B.R., 2019. Spatial distribution of soil moisture index across Nepal: a step towards sharing climatic information for agricultural sector. Theor. Appl. Climatol. 137, 3089–3102.
Tan, C., Yang, J., Li, M., 2015. Temporal-spatial variation of drought indicated by SPI and SPEI in Ningxia Hui Autonomous Region, China. Atmosphere. 6, 1399–1421. https://doi.org/10.3390/atmos6101399.
Thornthwaite, C.W., 1948. An approach toward a rational classification of climate. Geogr. Rev. 38, 55–94.
Trenberth, K.E., Dai, A., Van Der Schrier, G., Jones, P.D., Barichivich, J., Briffa, K.R., Sheffield, J., 2014. Global warming and changes in drought. Nat. Clim. Chang. 4, 17–22.
Van der Schrier, G., Jones, P., Briffa, K., 2011. The sensitivity of the PDSI to the thornthwaite and penman-monteith parameterizations for potential evapotranspiration. J. Geophys. Res.-Atmos. 116.
Vicente-Serrano, S.M., 2006. Differences in spatial patterns of drought on different time scales: an analysis of the Iberian Peninsula. Water Resour. Manag. 20, 37–60.
Vicente-Serrano, S.M., Beguería, S., López-Moreno, J.I., 2010. A Multiscalar Drought Index Sensitive to Global Warming: the standardized Precipitation Evapotranspiration Index. J. Clim. 23, 1696–1718. https://doi.org/10.1175/2009jcli2909.1.
Wang, S.-Y., Yoon, J.-H., Gillies, R.R., Cho, C., 2013. What Caused the Winter Drought in Western Nepal during recent years?*, +. J. Clim. 26, 8241–8256. https://doi.org/10.1175/jcli-d-12-00800.1.
Wang, Y., Zhang, J., Guo, E., Dong, Z., Quan, L., 2016. Estimation of variability characteristics of regional drought during 1964–2013 in Horqin Sandy Land China. Water. 8, 543. https://doi.org/10.3390/w8110543.
Watanabe, T., Yamazaki, K., 2014. Decadal-scale variation of south Asian summer monsoon onset and its relationship with the Pacific decadal oscillation. J. Clim. 27, 5163–5173.
Wilhite, D.A., Glantz, M.H., 1985. Understanding: the drought phenomenon: the role of definitions. Water Int. 10, 111–120.
Yang, M., Yan, D., Yu, Y., Yang, Z., 2016. SPEI-Based Spatiotemporal Analysis of Drought in Haihe River Basin from 1961 to 2010. Adv. Meteorol. 2016, 1–10. https://doi.org/10.1155/2016/7658015.
Yao, S., Sun, Q., Huang, Q., Chu, P., 2016. The 10–30-day intraseasonal variation of the East Asian winter monsoon: the temperature mode. Dyn. Atmos. Oceans 75, 91–101. https://doi.org/10.1016/.dynatmoce.2016.07.001.
Zargar, A., Sadiq, R., Naser, B., Khan, F.I., 2011. A review of drought indices. Environ. Rev. 19, 333–349. https://doi.org/10.1139/a11-013.